The theoretical expression (12) of the transfer coefficients enabled us to verify the consistency of the proposed steps with the experimental results

$$\overleftarrow{\alpha} = \overleftarrow{\gamma}/\nu + \beta r = 1.5$$

and

$$\vec{\alpha} = \vec{\gamma}/\nu + r - r\beta = 0.5$$

with $\overleftarrow{\gamma}$ being the number of steps previous to the controlling one, $\vec{\gamma}$ the number of steps after the controlling one, r the number of electrons transferred in that step, and β the symmetry coefficient.

Derivation of log of Eq. [19] for high anodic overpotentials leads to

$$B_a = \left(\frac{\partial \log E}{\partial \log i}\right)_{C_{HSO_3^-}} = \frac{2.303}{1.5}\frac{RT}{F} = 40 \text{ mV}$$

which is in good agreement with the experimental value of the Tafel slope. Equation [19] also fits the anodic reaction order in HSO_3^-.

Cathodic curves in the presence of O_2 were also determined to complete the analysis of the reactions occurring during the atmospheric corrosion of Zn. The limiting current for the O_2 reduction increased with the concentration of the salt, as can be seen in Fig. 3, indicating the positive effects of the anion, as it was also observed for NO_3^- for the O_2 reduction on Zn (13). The variation of the limiting current i_L for O_2 reduction with the anion concentration

$$\frac{\partial \log i_L}{\partial \log [HSO_3^-]} = 0.65$$

indicates that the reaction is under diffusion control at which a reaction overpotential is superposed with a heterogeneous reaction order 0.65 in the anion concentration.

For this reason, mechanistic conclusions cannot be obtained. The O_2 reduction would depend on the coverage of the electrode by the adsorption complex formed.

Conclusions

From the results presented here, the following can be concluded.

1. The Tafel constants and corrosion rate obtained from the POLCURR program in the vicinity of the corrosion potential are in good agreement with those extrapolated in the Tafel region.

2. In the absence of O_2, the Tafel constants and the reaction orders experimentally obtained for the anodic reaction, shown in Eq. [10] and [11], are in good agreement with the electrochemical parameters of the theoretical Eq. [19] derived on the base of an adsorption-oxidation sequence of reactions.

3. The controlling step in the oxidation of Zn is the charge transferrer reaction [14] giving as final product $ZnSO_3 \times 2\ 1/2\ H_2O$.

4. The O_2 reduction implies a heterogeneous reaction depending on the adsorption complex.

5. The overall reactions proposed, in aereated solutions are for

$$[HSO_3^-] < 5 \times 10^{-3} M$$

$$2Zn + 2HSO_3^- + 4H^+ \rightarrow S_2O_3^= + 2Zn^{++} + 3H_2O$$

and for

$$[HSO_3^-] > 5 \times 10^{-3} M$$

$$Zn + SO_2 + 1/2\ O_2 \rightarrow ZnSO_3$$

Manuscript submitted Jan. 6, 1984; revised manuscript received Feb. 18, 1985.

Instituto de Investigaciones Cientificas assisted in meeting the publication costs of this article.

REFERENCES

1. S. M. Gerchakov, L. R. Udey, and F. Mansfeld, *Corrosion*, **37**, 696 (1981).
2. C. Wagner and W. Traud, *Z. Elektrochem.*, **44**, 391 (1938).
3. M. Stern and A. L. Geary, *This Journal*, **104**, 56 (1957).
4. F. Mansfeld, *Corrosion*, **29**, 397 (1973).
5. D. M. Brasher, *Nature (London)*, **193**, 868 (1962).
6. D. M. Brasher, J. G. Beynon, A. D. Mercer, and J. E. Rhoades-Brown, in "Proceedings of the 2nd European Symposium on Corrosion Inhibition," p. 61, Ferrara, Italy (1965).
7. P. Berge, V. Jovancicevic, D. Noel, and P. Saint-Paul, *This Journal*, **129**, 2194 (1982).
8. E. T. Seo and D. T. Sawyer, *Electrochim. Acta*, **10**, 239 (1965).
9. A. Q. Contractor and H. Lal, *J. Electroanal. Chem. Interfacial Electrochem.*, **93**, 99 (1978).
10. V. K. Gouda, M. G. A. Khedr, and A. M. Shams el Dim, *Corros. Sci.*, **7**, 221 (1967).
11. E. Pouillard and J. P. Chiola, *Rev. Metall.*, **65**, 603 (1968).
12. J. O'M. Bockris and A. K. N. Reddy, "Modern Electrochemistry," Vol. 2, Plenum Publishing Corp., New York (1978).
13. B. M. Rosales, *Corros. Protec.*, **10**, 19 (1979).

Mechanical and Current Oscillations in Corroding Electrodes

O. Teschke,* F. Galembeck, and M. A. Tenan

Instituto de Fisica and Instituto de Química, Universidade Estadual de Campinas, 13100 Campinas, SP, Brasil

ABSTRACT

Mechanical oscillations of the solution meniscus risen around a corroding wire electrode were observed in synchronism with electrical current oscillations. Scanning electron microscopy coupled to microprobe analysis was used to investigate the topochemistry of the system under study. Solution capillarity effects on iron and on iron compounds are related to the oscillations detected in this system.

Iron corrosion by acids is a rather complex phenomenon (1-5), involving many steps of chemical and physical transformation of the system constituents. A recent work (6) shows that anodically polarized electrodes made of pure iron, immersed in sulfuric acid, are covered with ferrous salts; oxide formation occurs underneath these. The oscillatory phenomena observed during passivation of iron seems to be related to the formation and dissolution of salt films (7).

During experiments on the behavior of iron immersed in sulfuric acid solution, we have observed mechanical oscillations (*i.e.*, oscillatory vertical movement of sulfuric acid solution touching an iron tip, anodically polarized) coupled to electrical current oscillations. This observation suggests that capillary phenomena may be relevant to understand the behavior of passivating systems, at least in the case of incompletely immersed metal. The interpretation of capillary effects requires information on the topochemistry of the system under study, for which reason we have used scanning electron microscopy cou-

* Electrochemical Society Active Member.

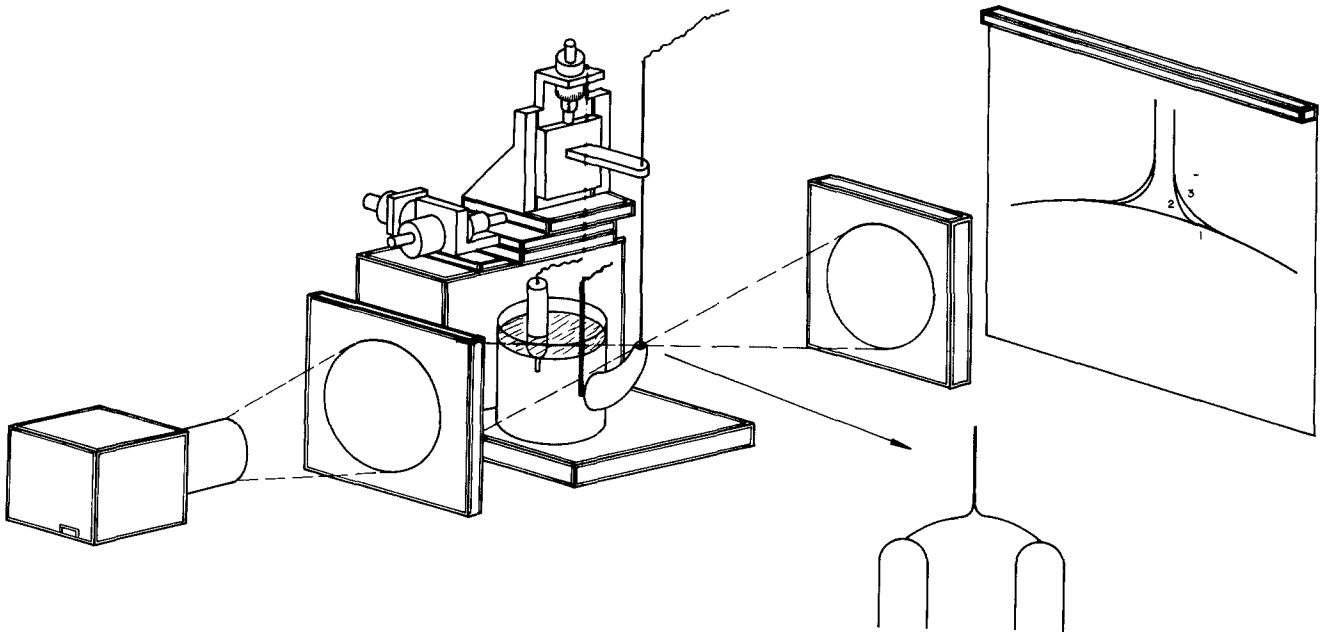

Fig. 1. Experimental setup

pled to microprobe analysis to examine corroding iron electrode. Results of these experiments are reported in this paper.

Experimental

The apparatus in which oscillations were observed consists of a borosilicate glass cylinder (8 cm diam, 15 cm height) as shown in Fig. 1. There is a lateral tubing (5 mm id at its top) exiting the cylinder. The cylinder volume is at least 100 times bigger than the capillary tube volume. A convex meniscus at the wetted capillary end (see detail in Fig. 1) was obtained by keeping the liquid level in the main cylinder a few millimeters above the meniscus level.

Reagent-grade chemicals were used without further purification. 1*N* aqueous H_2SO_4 was prepared using twice-distilled water. A 99.99% pure (C. Erba) iron wire 0.3 mm thick, cleaned with methanol and rinsed with twice-distilled water, was used as anode.

The iron electrode was grounded. Voltage was applied between the counterelectrode, a platinum wire with a downed area of at least 20 times larger than the area of the iron tip, and a saturated calomel electrode (SCE). An operational amplifier-based potentiostat kept the electrode voltages at the desired level, independent of the current. A constant voltage of +300 mV was applied between the iron electrode and the SCE. The current-time curves were recorded on a 7100 BM Hewlett-Packard Strip Chart Recorder. The photographs of the liquid level changes were taken using a Nikkon F-2 reflex camera fitted with extension tubes for greater magnification. In order to obtain reproducible current-time curves, it was necessary to use a fresh solution and a new iron electrode tip for each experiment.

The topography and composition of deposits formed during iron corrosion were examined using a scanning electron microscope. The pictures were obtained by secondary electron imaging, and the composition by x-ray microanalysis using a beam energy of 20 keV. The data reduction was made by a computer correction program. Since the x-rays producing regions in the sample are about 2 μm wide, it was possible to characterize different regions of the surface. The results obtained were then related to the most likely compounds of iron, sulfur, and oxygen to identify the substance in each point analyzed.

Results

A typical current-time oscillation is given in Fig. 2. It was observed that the oscillation period depends on the applied voltage, the diameter of the iron tip, and the radius of curvature of the liquid surface. Oscillation periods for other radii of curvature of the liquid surface were measured, but the results reported here are for a tube diameter of 5 mm (id).

It was found that the peak maximum was affected by a number of physical factors including magnetic stirring of the solution, concentration, shape of the conducting (iron) tip, and the exact placement of the iron tip with respect to the liquid interface. In the experiments reported here, the iron wire was cut normal to its axis. The iron tip was placed approximately at the center of the liquid meniscus, and it was positioned to touch the liquid surface gently by using micromanipulators. By capillary action, the liquid rises immediately, wetting the lower part of the iron electrode.

After an induction period of a few minutes, mechanical oscillations of the liquid level around the iron electrode are observed. The oscillation occurs between the levels shown in Fig. 3a and 3b. These oscillations are sustained for periods of up to 1h with changes of frequency and pulse amplitude.

The measured solution electrolyte contact angle on a surface covered with iron sulfate is approximately 30°, and for an oxide-covered metallic iron surface this is approximately 83° (measured directly from photograph prints). This change in the contact angle for the initial and final product of the electrode reaction indicates a considerable change in the iron tip wetting ability as it is cor-

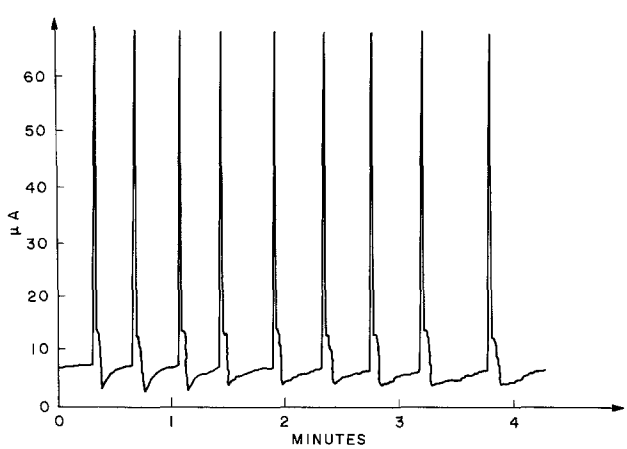

Fig. 2. Current-time profile for an iron electrode in a solution 1*N* of H_2SO_4 at constant external potential (300 mV SCE).

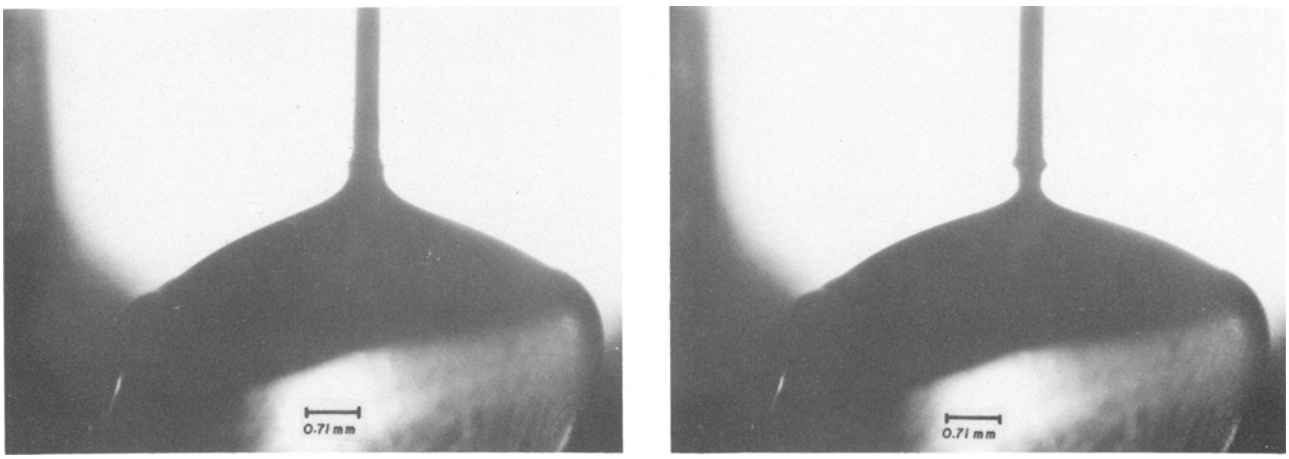

Fig. 3. Photograph of the liquid level changes at the iron electrode tip. a(left): Lower level. b(right): Upper level

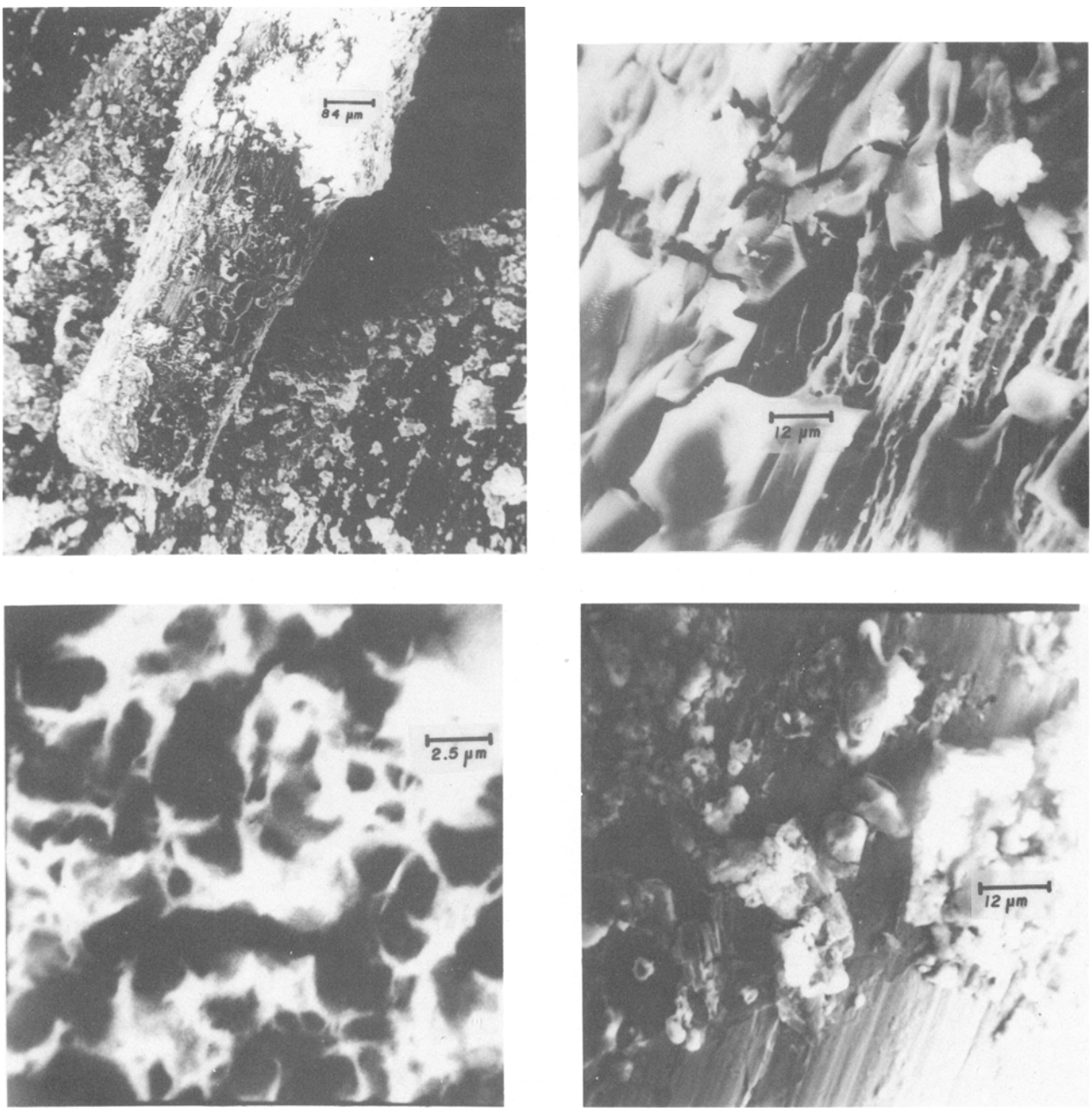

Fig. 4. SEM photograph of an iron tip. a(top left): Low amplification photograph showing the base iron (or oxide covered iron) as dark regions covered by a lighter overlayer of iron sulfate. b(top right): A detailed view of the drowned area of iron wire. c(bottom left): Oxide layer found under a crystal of iron sulfate removed in the SEM. d(bottom right): A detailed view of iron wire surface above the meniscus upper level.

roded by sulfuric acid. Note that these angles cannot be observed in Fig. 3 because the shape of the iron tip is being continuously altered by corrosion.

After some oscillations, the iron tip was gently removed from the solution and dried in air. SEM photographs were taken from these samples showing in detail the microstructure of the product formed at the movable air-liquid-metal interline.

A corroded iron tip is pictured in Fig. 4a. It is partly covered with thick pieces of light material appearing as bright, white areas. This material is also spread along the iron wire which was in contact with the solution, as shown in Fig. 4b. Microprobe analysis showed this material to contain iron and sulfur in different proportions: 9.52 atomic percent (a/o) Fe and 10.72 a/o S (Fe:S ratio ~ 1), and 19.32 a/o Fe and 12.70 a/o S (Fe:S ratio ~ 3:2). These two different measured Fe:S ratios may correspond to $FeSO_4 \cdot nH_2O$ and $Fe_3(OH)_1(SO_4)_2$, respectively, or could be attributed to the different compactness presented by the sample in different regions. This is a low conductivity solid which acquires charge under the SEM beam. It is possible to remove chunks of this material by allowing the sample to stay for some time under the beam. Under the iron sulfate pieces, we find the material shown in Fig. 4c, appearing as white, patched areas. From microprobe analysis, we obtained a composition of 52 weight percent (w/o) Fe and only *ca.* 1 w/o S. This material has a composition corresponding to that of hydrous iron (III) oxide. The dark product below this oxide layer is pure iron (95+ %, perhaps covered with an oxide layer much thinner than the microprobe sampling depth).

Examination of another area which corresponds to a point above the liquid-iron-air line, shown in Fig. 4d shows three main features: (*i*) bright spots which contain 20.73 a/o Fe and 13.27 a/o S (Fe:S ratio ~ 3:2), (*ii*) dark, rough areas (24 w/o Fe, 0.88 w/o S), and (*iii*) dark, even areas (100% Fe). From the microprobe analysis data, it is clear that the flat areas are made of bare metal. The highly reflecting areas are rich in iron sulfate, and the dark, rough areas contain less sulfate than the former; their composition corresponds to that of an hydrous iron oxide contaminated with some sulfate mixture. The features described above were found in other samples, but in many instances bare metal was not detected. Varying Fe:S ratios were frequently observed, indicating the occurrence of phases containing different proportions of oxide and sulfate.

Figure 5 shows a SEM photograph of the morphology of an area of the iron wire produced by the movement of the liquid-iron-air boundary. The iron wire was removed from the solution a few minutes after the mechanical oscillations started. The dark region (iron or iron oxide) surrounded by the lighter overlayer of iron sulfate was located just on the triple-phase boundary for the meniscus upper level. The dark area shown had its layer of iron sulfate removed by the liquid fall.

Discussion

From the results reported here, some conclusions may be drawn: (*i*) iron sulfate precipitates on mechanically oscillating iron electrodes, forming rather large crystals which tend to bulge out of the surface, instead of making films; (*ii*) other deposits are found which still contain some sulfate (perhaps as the result of adsorption or absorption in amorphous iron hydroxide); these are neither as prominent, nor as strongly insulating (at least regarding their ability to acquire electrostatic charge in the SEM beam); (*iii*) bare metal may also be detected, contiguous to areas covered with salt and oxide. However, this occurs less frequently than the other features found. Oxide films were found to form a porous layer under the iron sulfate in agreement with another recent report (6); (*iv*) the liquid-iron-air line movement removes the iron sulfate layer from the iron wire lateral surface, producing a region of bare metal.

The following mechanism is then proposed to justify the mechanical oscillations of the liquid level.

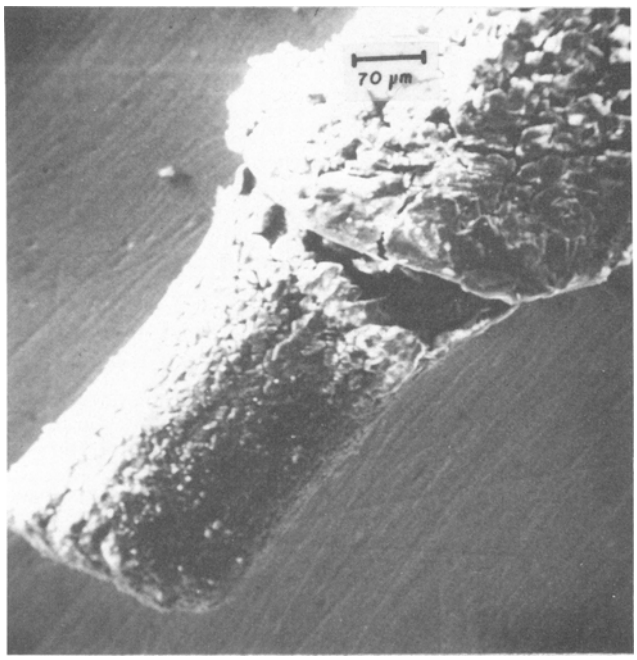

Fig. 5. SEM photograph of an iron tip removed from the solution a few minutes after mechanical oscillations started. The dark region (iron or iron oxide) surrounded by the lighter overlayer of iron sulfate was located just on the triple-phase boundary for the meniscus upper level.

1. Fe^{2+} ions are generated at the surface of the corroding positive electrode.

2. Metal oxidation is accompanied by a slow rise of the liquid level because the reaction products deposited on the metal surface are more hydrophilic than the metal itself. This resulting change in the contact angle for the initial and final product at the electrode surface plays an important role in the oscillation phenomenon. As can be seen from the equation for the total weight W of a liquid column rising above a flat liquid surface

$$2\pi\rho g \int_r^\infty h(x)x\,dx = W = 2\pi r\,\gamma\cos\theta \qquad [1]$$

(where the integration variable x represents the radial distance from the wire axis), the static equilibrium height $h(x = r)$ attained by the meniscus above the liquid surface is expected to be (*i*) an increasing function of both the wire radius r and the liquid-air surface tension γ and (*ii*) a decreasing function of the solid-liquid contact angle θ. According to Eq. [1], a change in the wettability conditions of the solid wall corresponding to a contact angle change from 80° to 30° leads to a fourfold increase in the weight of the liquid column supported by capillary action. The change in the exposed area of the electrode wire as suggested by this considerable weight increase can thus be responsible for the current rise prior to the current pulse. Figure 2 shows this increase of *ca.* 125% measured from the minimum current at the end of the sharp peak to the beginning of the next one. In analogy to liquid flow in cylindrical capillaries (8, 9), we can estimate for the conditions found in our experiments a time of a few seconds for the meniscus to attain its maximum height. This corresponds to the time of the slow rise of the current before the current pulse (see Fig. 2). Consequently, meniscus oscillations and current oscillations fit into the same time frame.

3. The liquid level oscillates between lower level and upper level shown in Fig. 3a and 3b. The liquid is at the upper level at the beginning of the current pulse. The liquid level stays at this position only for a very short period. Then the liquid falls rapidly, removing from the iron metal surface the iron solid compounds and forming a visible stream of solid products. As the solid layer falls off, the new bare metal surface reacts with the draining solution generating a current pulse. Figure 2a (lower

level) shows the position corresponding to the current minimum.

4. The time of the slow rise of the meniscus determines the spacing between current pulses, as shown in Fig. 1, and it increases after each oscillation. This is a consequence of the removal of the lateral cylindrical surface material by corrosion. The removal is faster at the tip in contact with the liquid. The iron corroded surface is gradually cone shaped in the successive motion steps until, finally, the liquid loses contact with iron electrode. At this point, the iron tip diameter has decreased so much that the surface tension forces are unable to stop the liquid downward movement (*cf.* Eq. [1]).

Conclusion

The meniscus oscillations described herein are induced by the combined action of three phenomena: capillarity of the liquid on the wire wall, wetting changes on the wire surface due to chemical reaction, and gravity. The iron oxidation reaction produces changes in the physical and chemical characteristics of the substrate solid surface, making the electrode wall more hydrophilic, up to the moving triple-phase boundary of the meniscus. Capillarity is thus responsible for the meniscus rise around the vertical wire. Gravity, on the other hand, is responsible for the liquid fall when, due to the poor wetting character of the iron surface at which oxide was converted to sulfate, the liquid-metal adhesion force is not sufficient to hold the liquid column.

Mechanical oscillations and current oscillations at an anodically polarized iron tip are thus interdependent for the system described. They are related to the formation and destruction of passivating oxide films. We believe that these findings should be relevant to the understanding of metal corrosion at liquid-air-metal intersection lines.

Manuscript submitted Sept. 12, 1984; revised manuscript received Jan. 23, 1985.

Universidade Estadual de Campinas assisted in meeting the publication costs of this article.

REFERENCES

1. D. A. Vermilyea, in "Advances in Electrochemistry and Electrochemical Engineering," Vol. 3, P. Delahay and C. W. Tobias, Editors, John Wiley and Sons, New York (1963).
2. T. P. Hoar, in "Modern Aspects of Electrochemistry," Vol. 2, J. O'M. Bockris, Editor, Butterworths, London (1959).
3. H. S. Isaacs and R. C. Newman, in "Corrosion and Corrosion Protection," R. P. Frankenthal and F. Mansfeld, Editors, p. 121, The Electrochemical Society Softbound Proceeding Series, Pennington, NJ (1981).
4. G. Kortum, "Treatise on Electrochemistry," 2nd ed., Elsevier, New York (1965).
5. J. R. Galvele, in "Treatise on Materials Science and Technology," Vol. 23, J. C. Scully, Editor, Academic Press, London (1983).
6. T. R. Beck, *This Journal*, **129**, 2412 (1982).
7. J. Wojtowicz, in "Modern Aspects of Electrochemistry," Vol. 8, B. E. Conway and J. O'M. Bockris, Editors, Chap. 4, Plenum Press, New York (1972).
8. E. W. Washburn, *Phys. Rev.*, **17**, 273 (1921).
9. G. Beni and M. A. Tenan, *J. Appl. Phys.*, **52**, 6011 (1981).

Current and Potential Transients during Localized Corrosion of Stainless Steel

Hugh S. Isaacs* and Yuichi Ishikawa[1]

Brookhaven National Laboratory, Upton, New York 11973

ABSTRACT

The currents flowing from a localized corrosion site (LCS) on passive stainless steel in air-saturated 0.25*M* NaCl have been studied using a vibrating probe electrode. The potential behavior during applied currents was analyzed by assigning equivalent circuits to the passive surface and the localized site so that the paths of the current across the passive surface and the LCS could be calculated and compared with the measured values. The equivalent circuit of the passive surface without active localized corrosion was determined from potential transients and was found to be dependent on the prior history of the electrode. The LCS was equated to a resistance with an EMF which were calculated from the LSC current and specimen potential. The variations of this resistance were attributable to changes in solution resistance adjacent to the LCS. It was found that the capacitance of the passive surface played a major role during potential transients and the initiation of pitting.

Potential fluctuations, observed during open-circuit exposure of stainless steels (1-5) and other passive metals (6-8) have been associated with the onset of chloride-induced localized corrosion. The potential of the passive metal depends on the behavior of both the freely exposed surface and the growing localized corrosion site (LCS). Under freely corroding conditions with rapid cathodic kinetics, for example, in ferric chloride solutions, the potential variations are determined by the polarization of this reaction. When these cathodic polarization currents are known, the corrosion rate can be determined directly from the potential (5). The potential has been observed to decrease relatively slowly when pits initiate and grow, but increase almost immediately when they repassivate in these solutions (4, 5). In contrast, when the cathodic reaction is slow, as with dissolved oxygen, the behavior becomes more complex. The potential then drops rapidly during the onset of pitting and increases slowly following repassivation (1-3, 6). The causes of the potential variations have not been presented in detail.

This work describes an approach to this problem which also closely resembles the exposures to which stainless steels are generally subjected. The approach developed from an analysis of results obtained with a scanning vibrating probe which has been used to monitor current from a LCS and leads to a number of interesting conclusions and possible applications.

Experimental

The location and monitoring of the currents from localized corrosion sites was accomplished using a scanning vibrating electrode. This technique was developed by biologists to overcome the noise interfering with amplification by masking small dc voltages (9, 10). The specific frequency of vibration enabled other signals associated with the noise to be filtered out and signals of the order of a few nanovolts to be measured (10). The design used

* Electrochemical Society Active Member.
[1] Visiting Scientist from Hitachi Limited, Mechanical Engineering Research Laboratory, Tsuchiura 300, Japan.